THE JOURNAL OF BIOLOGICAL CHEMISTRY VOL. 287, NO. 18, pp. 15087–15099, April 27, 2012

Disabled-2 Protein Facilitates Assembly Polypeptide-2-independent Recruitment of Cystic Fibrosis Transmembrane Conductance Regulator to Endocytic Vesicles in Polarized Human Airway Epithelial Cells*

Received for publication, January 11, 2012, and in revised form, March 5, 2012 Published, JBC Papers in Press, March 7, 2012, DOI 10.1074/jbc.M112.341875

Kristine M. Cihil[‡], Philipp Ellinger[§1], Abigail Fellows[§], Donna Beer Stolz[¶], Dean R. Madden[§], and Agnieszka Swiatecka-Urban[‡¶2]

From the [‡]Department of Nephrology, Children's Hospital of Pittsburgh, Pittsburgh, Pennsylvania 15224, the [§]Department of Biochemistry, Dartmouth Medical School, Hanover, New Hampshire 06902, and the [¶]Department of Cell Biology and Physiology University of Pittsburgh School of Medicine, Pittsburgh, Pennsylvania 15201

Background: The proteins that control CFTR endocytosis in epithelial cells have only been partially explored.
Results: In human airway epithelial cells Disabled-2 mediates recruitment of CFTR to clathrin-coated vesicles (CCVs) independent of the assembly polypeptide-2 (AP-2).
Conclusion: AP-2 is not essential for CFTR recruitment to CCVs in these cells.
Significance: Regulating CFTR interaction with Dab2 may stabilize CFTR in the plasma membrane.

Cystic fibrosis transmembrane conductance regulator (CFTR) is a cAMP-activated Cl^- channel expressed in the apical plasma membrane of fluid-transporting epithelia, where the plasma membrane abundance of CFTR is in part controlled by clathrin-mediated endocytosis. The protein networks that control CFTR endocytosis in epithelial cells have only been partially explored. The assembly polypeptide-2 complex (AP-2) is the prototypical endocytic adaptor critical for optimal clathrin coat formation. AP-2 is essential for recruitment of cargo proteins bearing the *YXXΦ* motif. Although AP-2 interacts directly with CFTR *in vitro* and facilitates CFTR endocytosis in some cell types, it remains unknown whether it is critical for CFTR uptake into clathrin-coated vesicles (CCVs). Disabled-2 (Dab2) is a clathrin-associated sorting protein (CLASP) that contributes to clathrin recruitment, vesicle formation, and cargo selection. In intestinal epithelial cells Dab2 was not found to play a direct role in CFTR endocytosis. By contrast, AP-2 and Dab2 were shown to facilitate CFTR endocytosis in human airway epithelial cells, although the specific mechanism remains unknown. Our data demonstrate that Dab2 mediates AP-2 independent recruitment of CFTR to CCVs in polarized human airway epithelial cells. As a result, it facilitates CFTR endocytosis and reduces CFTR abundance and stability in the plasma membrane. These effects are mediated by the DAB homology domain. Moreover, we show that in human airway epithelial cells AP-2 is not essential for CFTR recruitment to CCVs.

The cystic fibrosis transmembrane conductance regulator (CFTR)[3] belongs to the family of ATP binding cassette (ABC) transporters but forms a cAMP-activated Cl^- channel that mediates transepithelial Cl^- secretion in various fluid-transporting epithelia (1–3). In the airway CFTR plays a critical role in regulating mucociliary clearance by maintaining the airway surface liquid (4, 5). CFTR-mediated Cl^- secretion across polarized epithelial cells is modulated at the level of both channel activity and abundance in the plasma membrane (for review, see Refs. 6 and 7). The plasma membrane abundance of CFTR depends on its biosynthetic processing and post-maturational trafficking (for review, see Ref. 8). The long plasma membrane stability of CFTR stands in contrast to its inefficient biosynthetic processing and depends primarily on efficient recycling to compensate for rapid endocytosis, which occurs in clathrin-coated vesicles (CCV) (9, 10).

In addition to defective processing, post-maturational trafficking is also critically affected by the most common disease-associated mutation in the CFTR gene. In 70% of patient alleles, loss of Phe-508 (ΔF508) leads to a temperature-sensitive processing defect in the CFTR protein (for review, see Ref. 8). The temperature-rescued ΔF508-CFTR is partially functional as a Cl^- channel, but it is unstable in the plasma membrane due to altered endocytic trafficking (11, 12). Hence, understanding regulation of CFTR stability in the plasma membrane is critical

* This study was supported by National Institutes of Health Grants R01HL090767 and R01HL090767-02S1 (to A. S.-U.) and Grant R01DK075309 (to D. R. M.). This work was also supported by the Pennsylvania Department of Health, Health Research Formula Fund to the Children's Hospital of Pittsburgh of the University of Pittsburgh Medical Center Health System (to A. S.-U.) and a Hitchcock Foundation Program Project Grant (to D. R. M.).

[1] Present address: Institute of Biochemistry, Heinrich Heine University Düsseldorf, Germany.

[2] To whom correspondence should be addressed: Agnieszka Swiatecka-Urban, Children's Hospital of Pittsburgh, Department of Nephrology. Tel.: 412-692-9441; Fax: 412-692-8906; E-mail: asurban@pitt.edu.

[3] The abbreviations used are: CFTR, cystic fibrosis transmembrane conductance regulator; CCV, clathrin-coated vesicle; Dab2, Disabled-2; AP-2, assembly polypeptide-2; LDLR, low density lipoprotein receptor; DH, DAB homology; EGFR, epidermal growth factor receptor; IBMX, isobutylmethylxanthine; *F**-, N-terminal fluorescein; APP, amyloid precursor protein; PNS, post-nuclear supernatant.

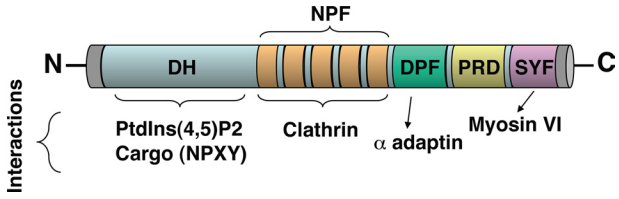

FIGURE 1. **Schematic illustration of domain organization in Dab2.** *DH*, DAB homology domain. Different regions in the DH domain interact directly with the plasma membrane phosphatidylinositol 4,5-diphosphate and the NP*X*Y motif in cargo proteins. The NPF repeats bind clathrin and assist in clathrin assembly. The DPF motif interacts with the α-adaptin of AP-2. *PRD*, proline-rich region. The SYF motif interacts with myosin VI and recruits myosin VI to endocytic sites at the plasma membrane.

to learn how to correct the endocytic trafficking defects of rescued ΔF508-CFTR.

Complex protein networks control the post-maturational trafficking of CFTR, which involves endocytic uptake followed either by recycling to the plasma membrane or by lysosomal degradation (7). Recent studies have shown that the plasma-membrane half-life and cell-surface abundance of CFTR can be stabilized by inhibition of the CFTR-associated ligand CAL or by depletion of the ubiquitin ligase c-Cbl (13, 14). Although several proteins involved in the uptake process have been identified (15), their roles are incompletely defined in polarized airway epithelial cells. As a result, selective trafficking processes of CFTR remain elusive.

Clathrin-mediated endocytic uptake requires two closely related but distinct processes. The first involves the assembly of the clathrin coat, and the second requires recruitment of cargo proteins to the site of endocytosis for incorporation into CCVs. The assembly polypeptide-2 (AP-2), a heterotetrameric complex of the α, β2, σ2, and μ2 adaptins, is the prototypical endocytic adaptor with key roles in both processes (for review, see Ref. 16). Three of the AP-2 adaptins (α, β2, and σ2) participate directly in clathrin coat assembly. The μ2 adaptin binds directly to the Y*XX*Φ motifs in transmembrane cargo proteins. As a result, depletion of AP-2 by more than 90% results in a 10-fold reduction of CCV number. This profoundly inhibits the endocytic uptake of cargo proteins that rely entirely on the Y*XX*Φ motif, such as the transferin receptor (TfR), but has very little effect on the uptake of other clathrin cargo proteins, such as the low density lipoprotein receptor (LDLR) (17). Alternative adaptor proteins mediate privileged cargo recruitment independent of μ2, enabling proteins such as LDLR to maintain efficient internalization even when the number of CCVs is strongly depleted (17).

AP-2 has clearly been shown to play a role in CFTR endocytosis in cells that endogenously express the channel (14, 18, 19). In non-epithelial cells, AP-2 is necessary for efficient CFTR endocytosis, and the μ2 adaptin interacts directly with the CFTR YDSI motif *in vitro* (10, 20, 21). Thus, in HEK293 cells, even a modest 64% knockdown of α-AP-2 caused a 2-fold reduction in the endocytic uptake of CFTR (18). In comparison, the situation in airway epithelial cells is less clear. The μ2 knockdown by more than 90% resulted in only a 2-fold reduction in CFTR endocytosis compared with the dramatic reduction seen for purely Y*XX*Φ-mediated uptake (17, 19). Furthermore, several distinct endocytic motifs were found in the C-terminal tail of CFTR (22), suggesting that AP-2 may not be obligatory for CFTR recruitment to CCVs in airway epithelia.

Disabled-2 (Dab2) is a clathrin-associated sorting protein (CLASP) that, like AP-2, facilitates endocytosis by organizing clathrin assembly and by recruiting cargo and other adaptor proteins (for review, see Ref. 16). The Dab2 DAB homology (DH) domain binds to the plasma membrane phosphatidylinositol 4,5-diphosphate, whereas the Dab2 NPF sequence repeats assist in clathrin assembly (Fig. 1). Moreover, the DH domain binds cargo proteins containing the NP*X*Y motif. Thus, Dab2 can sustain endocytosis of NP*X*Y-containing proteins, such as LDLR even when CCV number is limiting (17). Dab2 can also promote endocytosis by binding directly via its DPF domain to the α-adaptin and working in concert with AP-2 (Fig. 1).

Three published studies have implicated Dab2 in CFTR endocytosis. CFTR co-immunoprecipitated with Dab2 and myosin VI in human airway epithelial cells (23) and colocalized with Dab2, AP-2, and myosin VI in rat enterocytes (18). CFTR abundance was increased in the intestines of Dab2 KO mice, and CFTR endocytosis was inhibited after Dab2 depletion in human airway epithelial cells (18, 19). However, little is known about the specific mechanism whereby Dab2 facilitates CFTR endocytosis. CFTR does not contain a canonical NP*X*Y motif, and it has thus been proposed that its role is dependent on interactions with AP-2 and/or other endocytic adaptors, such as myosin VI (18, 19). No published studies addressed directly whether Dab2 can recruit CFTR to clathrin coats independent of AP-2 and thus facilitate CFTR endocytosis in airway epithelial cells. Moreover, it remains to be determined whether AP-2 controls CFTR endocytosis primarily by clathrin coat assembly or whether it is also critical for CFTR recruitment to CCVs.

The goal of this study was to answer these questions. We report that in polarized human airway epithelial cells (CFBE41o-), Dab2 recruits CFTR to CCVs and mediates CFTR endocytosis by an AP-2 independent mechanism that requires the Dab2 DH domain. This is the first report that Dab2 controls CFTR endocytic recruitment by an AP-2-independent mechanism. Moreover, our data demonstrate that AP-2 is not essential for CFTR recruitment to CCVs in human airway epithelial cells. Because rescued ΔF508-CFTR has decreased plasma membrane stability, our data indicate that regulating the CFTR-Dab2 interaction may provide useful biochemical tools and a future pharmacological approach to stabilize the ΔF508-CFTR in the plasma membrane.

MATERIALS AND METHODS

Cell Lines and Cell Culture—CFBE41o- cells stably expressing wild type (WT)-CFTR and parental CFBE41o- cells were a generous gift from Dr. J. P. Clancy, Department of Pediatrics, University of Alabama at Birmingham, Birmingham, AL (24). WT-CFTR expressing CFBE41o- cells were seeded on Transwell (4.67 or 44 cm^2) or Snapwell (1.12 cm^2, 0.4-μm pore size; Corning Corp.) permeable supports coated with plating medium containing Dulbecco's modified Eagle's medium (Invitrogen) and 10% purified collagen (PureCol™; Advanced Biomatrix, San Diego, CA) and maintained as polarized monolayers in air-liquid interface culture as described previously

(14). CFBE41o- cells transfected with plasmid DNA were seeded on collagen-coated plastic tissue culture plates (Corning Corp.) and cultured for 72 h. FBS and the selection antibiotic were removed from the media 18 h before experiments to augment cell polarization and cell cycle synchronization (25, 26). The parental CFBE41o- cells were maintained under the same culture conditions but without puromycin (12).

RNA-mediated Interference—Transfection of CFBE41o- cells with siRNA (Qiagen, Valencia, CA) was conducted using HiPerFect Transfection Reagent (Qiagen) according to the manufacturer's instructions. The following human genes were targeted: Dab2 (siDab2; Hs_Dab2_6 siRNA), the μ2 adaptin (Hs_AP2M1_5, Hs_AP2M1_7, and Hs_AP2M1_8), the α-adaptin (Hs_AP2A2_4), ARH (Hs_ARH_1), or siRNA negative control (AllStars, non-silencing siRNA; siCTRL). A second siRNA, targeting another non-conserved region of the human Dab2 gene purchased from Qiagen (Hs_Dab2_5), also silenced the expression of Dab2 with similar efficiency. The Hs_Dab2_6 siRNA was used in subsequent experiments. CFBE41o- cells (1.0×10^6) were plated on tissue culture plates and incubated with the optimized transfection mixture containing 50 nM siRNA at 37 °C. After 24 h, cells were trypsinized and plated on collagen-coated Transwell or Snapwell-permeable supports and cultured for an additional 6 days to establish polarized monolayers (total 7 days in culture). All experiments were done under the same cell culture conditions to assure similar cellular polarization as well as protein expression and trafficking. Silencing the target genes under these conditions resulted in the corresponding protein depletion by ~60%. We aimed at such a level of silencing for two reasons; first, to allow sufficient clathrin coat formation to better differentiate the adaptors role in clathrin coat formation *versus* cargo recruitment, and second, to avoid off-target effects that may occur with more dramatic gene silencing.

Plasmids and Transient Transfection—The cDNAs encoding human full-length WT-CFTR and the CFTR Y1424A mutant in pS65T-C1 vector (GFP-CFTR WT and GFP-CFTR Y1424A, respectively) were generous gifts from Dr. Bruce A. Stanton, Department of Physiology, Dartmouth Medical School, Hanover, NH. Human Dab2 (Uniprot accession number P98082-1) was obtained from Origene (SC321375) Technologies, Inc., Rockville, MD). The Dab2 fragments expressing the DH domain were subcloned by PCR into the pEGFP-C1 vector (Clontech Laboratories, Inc., Mountain View, CA) using primers (IDT) encoding BsrGI and HindIII restriction enzyme sites (GFP-Dab2 DH). To construct the GFP-Dab2 DH S122T/H144F mutant (GFP-Dab2 DH 122/144) previously described (27), the GFP-Dab2 DH cDNA was mutated using the QuikChange™ II XL site-directed mutagenesis kit (Stratagene; La Jolla, CA). Constructs were sequence verified by ABI PRISM dye terminator cycle sequencing (Applied Biosystems, Foster City, CA). Transfection of cells with plasmids was performed using FuGENE 6 (Roche Diagnostics) according to the manufacturer's instructions.

Antibodies and Reagents—The following antibodies were used: anti-human CFTR (mouse monoclonal clone 596 (Cystic Fibrosis Foundation Therapeutics, Inc., Chapel Hill, NC (or M3A7 (Millipore, Billerica, MA)), anti-Dab2 (mouse monoclonal p96 (BD Biosciences)), rabbit monoclonal (Epitomics, Burlingame, CA), anti-GFP (mouse monoclonal JL8 or rabbit polyclonal (Clontech)), anti-clathrin heavy chain (mouse monoclonal (BD Biosciences)), anti-μ2 adaptin (mouse monoclonal AP50 (BD Biosciences)), chicken polyclonal AP2M1 (ProSci Inc., Powy, CA)), anti-α-adaptin (mouse monoclonal AP6; Thermo-Fisher), anti-autosomal recessive hypercholesterolemia protein (ARH; Abnova, Taipei, Taiwan), anti-epidermal growth factor receptor (EGFR) D38B1 (rabbit monoclonal (Cell Signaling Technology, Danvers, MA)) and anti-LDLR (rabbit monoclonal (Abcam, Cambridge, MA)), anti-ezrin (mouse monoclonal (BD Transduction Laboratories)), and anti-actin (mouse monoclonal AC-15 or rabbit polyclonal (Sigma)). Horseradish peroxidase-conjugated goat anti-mouse and goat anti-rabbit (Bio-Rad) secondary antibodies were used. All antibodies were used at the concentrations recommended by the manufacturer or as indicated in the figure legends.

Density Gradient Separation and Differential Centrifugation of CCV—To isolate CCVs, subcellular fractionation was performed by density gradient and differential centrifugation as described previously (28). After washing with ice-cold PBS at 4 °C, CFBE41o- cells were scraped in buffer A, pH 6.5, containing 1 M MES, 10 mM EGTA, and 0.5 M $MgCl_2$ and homogenized in a glass-Teflon homogenizer using 20 strokes at 1500 rpm. To prepare the microsomal fraction (P2)-containing CCVs, the homogenates were centrifuged at 17,000 $\times$ *g* for 20 min in a Sorvall Biofuge at 4 °C, and the resultant supernatant (S1) was centrifuged at 56,000 $\times$ *g* for 60 min at 4 °C in a Sorvall swinging bucket rotor TH641 in Sorvall WX 80 Ultra. The resultant pellet (P2) was resuspended in buffer A, homogenized with 5 strokes at 1500 rpm, fresh buffer A was added, and the suspension was passed through a syringe barrel equipped with a 27-gauge 5/8 in needle. To pellet CCVs through the sucrose cushion, the P2 suspension was collected in 12.2-ml polyallomer tubes (Sorvall, 14 mm diameter), and the D_2O-sucrose solution (8% w/v final) was injected at the bottom of the tube underneath the P2 suspension and centrifuged at 120,000 $\times$ *g* for 2 h at 4 °C in a Sorvall swinging bucket rotor TH641 in Sorvall WX 80 Ultra. After discarding the supernatant, the pelleted CCVs were resuspended in a small volume of buffer A and collected.

Immunogold Labeling—Copper grids (200 mesh) were coated with 0.125% Formvar (Ted Pella, Redding, CA) in chloroform. Washed CCVs (1–10 μl of suspension) were loaded onto grids for adsorption. Excess sample solution was wicked away with filter paper. For immunostaining, vesicles were fixed with 2% paraformaldehyde in PBS for 5 min. The vesicles were washed 3 times with PBS and then 3 more times with PBG (PBS with 0.5% BSA, 0.15% glycine). Samples were blocked by 30 min of incubation with 5% normal donkey serum in PBG. CCVs were labeled with rabbit anti-Dab2 (1:25), mouse anti-CFTR clone 596 (1:50), and chicken anti-μ2 AP2M1 (1:100) for 1 h at room temperature. Samples were washed 4 times with PBG and then labeled with secondary antibodies conjugated to colloidal gold (donkey anti-mouse 6 nm, donkey anti-chicken 12 nm, and donkey anti-rabbit 18 nm) all at 1:25 dilution at room temperature for 1 h. Sections were washed 3 times in PBG and three times in PBS. The sections were fixed in 2.5% glutaraldehyde in

PBS for 5 min, washed 2 times in PBS, and then washed 6 times in double distilled H_2O. Sections were post-stained in 2% neutral uranyl acetate for 7 min, washed 3 times in sterile H_2O, stained 2 min in 4% uranyl acetate, then embedded in 1.25% methyl cellulose. Labeling was observed on a JEOL JEM 1011 electron microscope (Peabody, MA) at 80 kV.

Biochemical Determination of Plasma Membrane CFTR—The biochemical determination of plasma membrane CFTR was performed by domain-selective plasma membrane biotinylation of cells grown on permeable growth supports or by cell-surface biotinylation of cells grown in tissue culture dishes. Treatment with EZ-Link™ Sulfo-NHS-LC-Biotin (Pierce) was followed by cell lysis in buffer containing 25 mM HEPES, pH 8.0, 1% Triton, 10% glycerol, 1 mM Na_3VO_4, and Complete Protease Inhibitor Mixture (Roche Applied Science) as described previously in detail (14, 29). Incubation of cells with cycloheximide (Sigma; 20 μg/ml), a protein synthesis inhibitor, was performed at 37 °C, and the disappearance of CFTR from the plasma membrane was monitored over time, as previously described (12). Biotinylated CFTR was visualized by Western blotting with mouse monoclonal antibody, clone 596, and an anti-mouse horseradish peroxidase antibody using the Western Lightning™ Plus-ECL detection system (PerkinElmer Life Sciences) followed by chemiluminescence. Quantification of biotinylated CFTR was performed by densitometry using exposures within the linear dynamic range of the film.

Endocytic Assay—Endocytic assays were performed in CFBE41o- cells as described previously (30, 31). Briefly, the plasma membrane proteins were first biotinylated at 4 °C using EZ-Link™ Sulfo-NHS-SS-Biotin (Pierce). Cells were rapidly warmed to 37 °C for 2.5, 5, 7.5, or 10 min after biotinylation, and subsequently the disulfide bonds on Sulfo-NHS-SS-biotinylated proteins remaining in the plasma membrane were reduced by l-glutathione (GSH; Sigma) at 4 °C. At this point in the protocol, biotinylated proteins reside within the endosomal compartment. Subsequently, cells were lysed, and biotinylated proteins were isolated by streptavidin-agarose beads, eluted into SDS sample buffer, and separated by 7.5% SDS-PAGE. The amount of biotinylated CFTR at 4 °C and without the 37 °C warming was considered 100%. The amount of biotinylated CFTR remaining in the plasma membrane after GSH treatment at 4 °C and without the 37 °C warming was considered background (5.6 ± 1.1% compared with the amount of biotinylated CFTR at 4 °C without GSH treatment) and was subtracted from the CFTR biotinylated after warming to 37 °C at each time point. CFTR endocytosis was calculated after subtraction of the background and was expressed as the percent of biotinylated CFTR at each time point after warming to 37 °C compared with the amount of biotinylated CFTR present before warming to 37 °C.

Ussing Chamber Measurements—Ussing chamber measurements were performed as previously described (32). Monolayers of airway cells grown on Snapwell-permeable supports were mounted in an Ussing-type chamber (Physiologic Instruments; San Diego, CA) and bathed in solutions (see below) maintained at 37 °C and stirred by bubbling with 5% CO_2, 95% air. Short circuit current (*I*sc) was measured by voltage-clamping the transepithelial voltage across the monolayers to 0 mV with a voltage/current clamp (model VCC MC8, Physiologic Instruments) as described previously (32). Data collection and analysis were done with Acquire & Analyze Data Acquisition System (Physiologic Instruments). CFBE41o- cells were bathed in solutions with an apical-to-basolateral Cl^- gradient in the presence of amiloride (100 μM) in the apical bath solution to inhibit Na^+ absorption. The apical bath solution contained 115 mM sodium gluconate, 5 mM NaCl, 25 mM $NaHCO_3$, 3.3 mM KH_2PO_4, 0.8 mM K_2HPO_4, 1.2 mM $MgCl_2$, 4 mM calcium gluconate, 10 mM mannitol, pH 7.4. The basolateral bath solution contained 120 mM NaCl, 25 mM $NaHCO_3$, 3.3 mM KH_2PO_4, 0.8 mM K_2HPO_4, 1.2 mM $MgCl_2$, 1.2 mM $CaCl_2$, 10.0 mM glucose, pH 7.4. A low Cl^-, high-Na^+, high gluconate, apical bath solution was used to prevent cell swelling due to the increased apical Cl^- permeability under these conditions, as previously described (32). *I*sc was stimulated with 20 μM forskolin, and 50 μM IBMX added to the apical and basolateral bath solution. Thiazolidinone $CFTR_{inh}$-172 (20 μM; Tocris Bioscience, Ellisville, MO) was added to the apical bath solution to inhibit CFTR-mediated *I*sc. Data are expressed as forskolin/IBMX stimulated *I*sc, calculated by subtracting the base-line *I*sc from the peak stimulated *I*sc.

Immunoprecipitation and Immunoblotting—CFTR was immunoprecipitated from cell lysates by methods described previously (12, 23). Briefly, cultured cells were lysed in an immunoprecipitation buffer containing 150 mM NaCl, 50 mM Tris, pH 7.4, 1% IGEPAL (Sigma), 5 mM $MgCl_2$, 5 mM EDTA, 1 mM EGTA, 30 mM NaF, 1 mM Na_3VO_4, Complete Protease Inhibitor Mixture and PhosSTOP (Roche Applied Sciences). After centrifugation at 14,000 × *g* for 15 min to pellet insoluble material, the soluble lysates referred to as post-nuclear supernatants (PNS) were precleared by incubation with protein G-Sepharose beads conjugated with the non-immune mouse IgG_1 (DAKO North America, Inc., Carpinteria, CA) (Pierce) at 4 °C. The pre-cleared lysates were added to the protein G-Sepharose bead antibody complexes. CFTR was immunoprecipitated by incubation with the mouse M3A7 antibody (IgG_1). After washing the protein G-Sepharose bead-antibody complexes with the immunoprecipitation buffer, immunoprecipitated proteins were eluted by incubation at 85 °C for 5 min in sample buffer (Bio-Rad) containing 100 mM DTT. Immunoprecipitated proteins were separated by SDS-PAGE using 7.5% gels (Bio-Rad) and analyzed by Western blotting. The immunoreactive bands were visualized with the Western Lightning™ Plus-ECL detection system.

Recombinant Dab2 Binding Assays—Human Dab2 (Uniprot accession number P98082-1) was obtained from Origene (SC321375) and subcloned by PCR into pET16b (Novagen) using the XhoI and BamHI restriction enzyme sites. Primers (IDT) were designed to include a 3C protease cleavage site (LEVLFQ↓GP) immediately after the XhoI recognition sequence and fused directly to residues 1–205 of the native protein containing the DH domain. The construct was verified by DNA sequencing. Protein was expressed in *Escherichia coli* BL21(DE3)RIL cells grown overnight at 20 °C in lysogeny broth after induction (0.1 mM isopropyl 1-thio-β-D-galactopyranoside) and purified using immobilized metal ion affinity (10-ml Ni-NTA Superflow; Qiagen) and size-exclusion (HiLoad Superdex 75 26/60 column; GE Healthcare) chromatography.

The polyhistidine tag was removed by 20 h incubation at 4 °C with human rhinovirus 3C protease (Novagen) at a 1:100 mass ratio. Tag-free protein was recovered in the flow-through of a 5-ml HisTrap HP column (GE Healthcare) and dialyzed into 25 mM Tris, pH 8.0, 150 mM NaCl, 1 mM DTT, 0.02% (w/v) NaN_3. Protein concentration was determined via A_{280} using a mass extinction coefficient of 0.62 calibrated by quantitative amino acid analysis (Keck Facility, Yale University). An APP10 reporter peptide (*F**-QNGYENPTYK) was synthesized with an N-terminal fluorescein (*F**-) and an amidated C terminus (Tufts University Core Facility).

Fluorescence intensity was measured using a Spectramax MD5 plate reader. Protein for all experiments was supplemented with 0.1 mg/ml bovine IgG (Sigma) and 0.5 mM Thesit (Fluka). A stock protein solution was serially diluted (~130 nM to 300 μM), and *F**-APP10 was added to a final concentration of 30 nM. Plates were allowed to equilibrate 15 min at 24 °C before measurement. Fitting was performed as described (13).

In Vivo F-APP10 Peptide Uptake*—Immunofluorescence staining and confocal microscopy studies were conducted to confirm the uptake of the *F**-APP10 peptide. CFBE41o- cells expressing WT-CFTR were cultured on semi-permeable growth supports in air-liquid interface for 7 days. FBS was withdrawn from the culture medium 24 h before the experiment. The *F**-APP10 peptide was prepared fresh as 167 mM stock in DMSO, diluted with PBS to 1.25 mM, and added to a BioPORTER® Protein Delivery Reagent tube (Sigma). Subsequently, the Opti-MEM medium was added to the BioPORTER complex containing the *F**-APP10 peptide, and the solution was warmed to 37 °C. The *F**-APP10 peptide or vehicle control (CTRL) was added to the apical chamber of monolayers and incubated for 30 min in the cell culture incubator at 37 °C. Subsequently, monolayers were thoroughly washed at 4 °C and fixed with 2% paraformaldehyde in PBS for 15 min. The monolayers were mounted onto slides with ProLong Gold Antifade reagent with DAPI (Invitrogen), and cells were imaged on an inverted FluoView 1000 confocal microscope (Olympus; Center Valley, PA) using the 60×, numerical aperture 1.42 oil immersion, as described above. The N-terminally located fluorescein tag on the internalized *F**-APP10 peptide was excited at 488 nm spectral line of the multiline argon laser. Additional, biotinylation experiments were performed after incubation of the CFBE41o- cells with the *F**-APP10 peptide or vehicle control to determine the plasma membrane abundance of CFTR and LDLR as described above.

Data Analysis and Statistics—Statistical analysis of the data were performed using GraphPad Prism Version 4.0 for Macintosh (GraphPad Software Inc., San Diego, CA). The means were compared by a two-tailed *t* test. A p value <0.05 was considered significant. Data are expressed as the mean ± S.E.

RESULTS

Dab2 Co-distributes with CFTR in CCVs in Polarized Human Airway Epithelial Cells—Little is known about the distribution of Dab2 in polarized epithelial cells. CFBE41o- cells stably expressing WT-CFTR and grown on semipermeable growth supports for 7 days were lysed, and the CCV fraction was isolated by density gradient and differential centrifugation. The

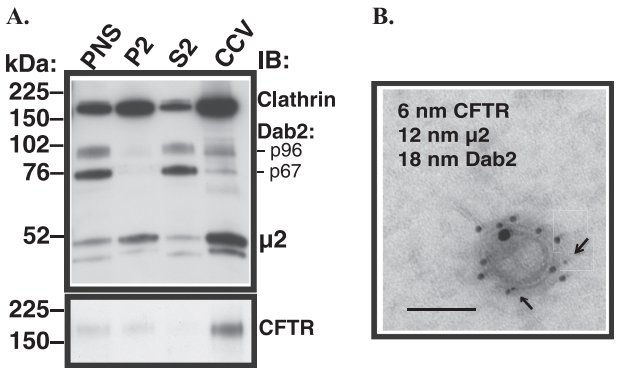

FIGURE 2. **Experiments demonstrating that Dab2 co-distributes with CFTR in CCV in polarized human airway epithelial cells.** *A*, representative Western blots (*IB*) demonstrate distribution of CFTR and endocytic adaptors in subcellular fractionations and CCVs in polarized CFBE41o- cells expressing WT-CFTR. Subcellular fractionation and isolation of CCVs was carried out by density gradient and differential centrifugation. Polarized CFBE41o- cells express two major spliceforms of Dab2 (*top panel*). The Dab2 p96 that plays a role in endocytosis co-distributed with clathrin, the μ2 adaptin, and with CFTR in CCVs. By contrast, the p67 spliceform that does not have a role in endocytosis was depleted from the CCV fraction. *P2*, cytosolic fraction; *S2*, microsomal fraction. Three experiments/group were performed. *B*, shown is a representative electron micrograph of a vesicle from the CCV fraction demonstrating that Dab2, μ2, and CFTR co-exist in the same CCV. The CCV fraction was fixed by incubation 1:1 with 4% paraformaldehyde, and vesicles were permeabilized and immunolabeled with antibodies conjugated to different sized gold particles. The *arrows* point to the smallest gold particles conjugated with the anti-CFTR antibody. *Error bar* = 50 nm. All experiments were repeated twice from separate cultures with similar results.

Dab2 gene is alternatively spliced to produce two proteins (33). Although the Dab2 p96 spliceform functions as an endocytic adaptor, the p67 spliceform does not have a role in endocytosis (34, 35). As illustrated in Fig. 2*A*, both Dab2 spliceforms were expressed in polarized CFBE41o- cells, but as expected, only the less abundant Dab2 p96 was enriched in the CCV fraction where it co-distributed with other CCV proteins, clathrin and the μ2 adaptin, and with CFTR. As demonstrated by immunogold electron microscopy, Dab2, μ2, and CFTR are found together in individual vesicles in the CCV fraction (Fig. 2*B*). The above data illustrate that Dab2 co-distributes with the plasma membrane clathrin coats and with CFTR in CFBE41o- cells.

Partial Silencing of Dab2, but Not AP-2, Increases Plasma Membrane Abundance and Stability of CFTR in Polarized CFBE41o- Cells—To examine the specific mechanism whereby AP-2 and Dab2 facilitate CFTR endocytosis in polarized airway epithelial cells, we used RNA mediated interference (siRNA). Previous studies have shown that depleting any one of the adaptins in the AP-2 complex decreases stability of the remaining subunits and that the partial complexes that form in the absence of a particular subunit are inactive and fail to localize to membranes (17, 36, 37). Because nearly complete depletion of AP-2 can affect both CCV formation and cargo recruitment (17), we aimed for a less profound inhibition of CCV formation to test the specificity of AP-2 in recruiting CFTR to CCVs in polarized human airway epithelial cells. A similar approach was previously used to test the role of AP-2 in non-epithelial systems (18). Because the μ2 adaptin is unique to AP-2, we therefore used a siRNA targeting a non-conserved region of the human μ2 adaptin gene (siμ2) to specifically inhibit AP-2 assembly.

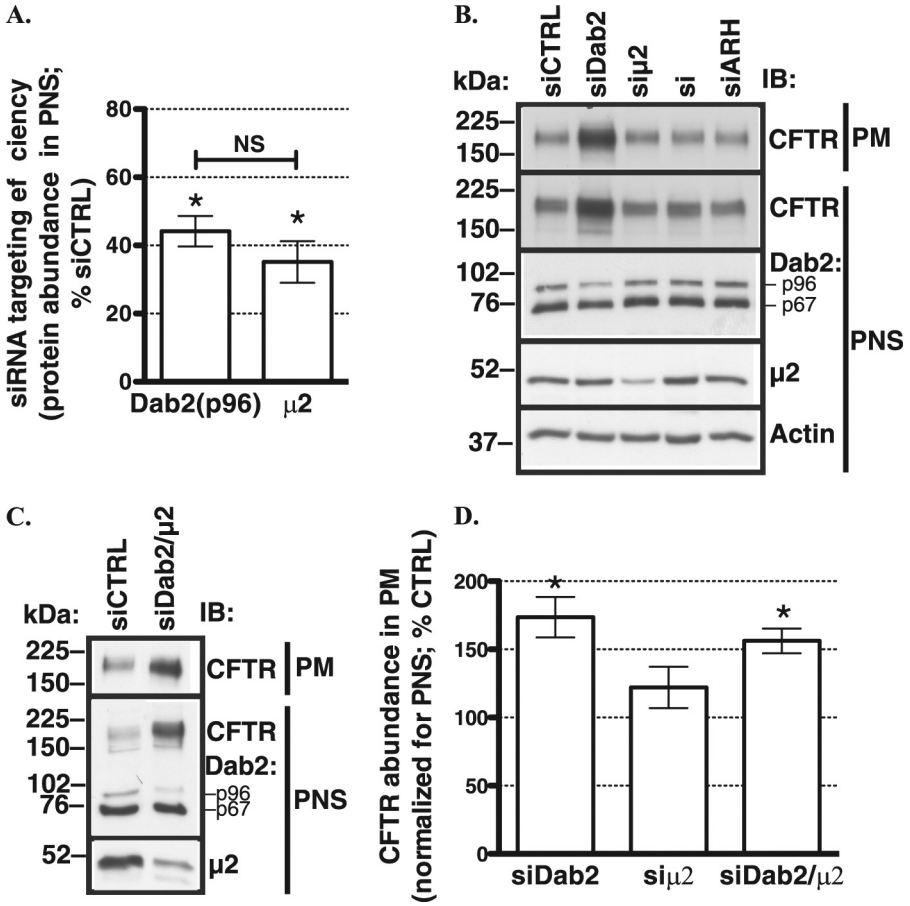

FIGURE 3. **Biotinylation experiments performed to determine the effects of Dab2 and AP-2 on CFTR abundance in polarized CFBE41o- cells.** Cells were transfected with 50 nM siRNA. The Dab2 gene is alternatively spliced to produce two proteins, p96 and p67 (33). Because the Dab2 p96 functions as an endocytic adaptor, it was specifically targeted by the siRNA. Silencing the μ2 adaptin was used to inhibit the AP-2 complex assembly. A summary of experiments (*A*) and representative Western blots (*IB*; *B*, *bottom three rows*) demonstrate that siDab2 decreased the Dab2 p96 protein abundance in PNS by ~60% without decreasing abundance of the μ2 adaptin. siμ2 decreased the μ2 protein abundance in PNS by ~60% without decreasing abundance of Dab2. Shown in *B* (*top two rows*) are the effects of siRNAs on CFTR abundance in the PNS and plasma membrane (*PM*). The plasma membrane abundance of CFTR was normalized for PNS CFTR (*D*). Silencing Dab2 but not the closely related protein adaptor, ARH, increased the steady-state plasma membrane abundance of CFTR in polarized CFBE41o- cells (*B* and *D*). By contrast, the plasma membrane abundance of CFTR did not increase after silencing the μ2 adaptin (*B* and *D*). Likewise, silencing the α-adaptin (siα) did not increase CFTR abundance in the plasma membrane (*B*). Silencing Dab2 and μ2 together increased the plasma membrane CFTR abundance, similar to silencing Dab2 alone (*C* and *D*). Plasma membrane proteins were isolated by selective apical membrane biotinylation, and the plasma membrane CFTR was normalized for PNS CFTR. Actin expression in PNS was used as a loading control. *, $p < 0.05$ *versus* siRNA negative control (siCTRL). Six experiments/group were performed. *Error bars*, S.E. *NS*, not significant.

In addition, to directly compare the role of Dab2 in CFTR endocytosis, its expression was reduced by targeting a non-conserved region of the human Dab2 (p96) sequence (siDab2). CFBE41o- cells stably expressing WT-CFTR were transfected with siμ2, siDab2, or with one of three controls: a non-silencing siRNA (siCTRL), siRNAs targeting the α-adaptin (siα), or the closely related to Dab2 protein adaptor ARH (siARH). Cells were cultured on semipermeable growth supports for a total of 7 days. siDab2 decreased the Dab2 p96 protein abundance in PNS by ~60% without decreasing the abundance of the μ2 adaptin (Fig. 3, *A* and *B*). Conversely, siμ2 decreased the μ2 protein abundance by ~60% without decreasing Dab2 abundance (Fig. 3, *A* and *B*).

Partial silencing of Dab2, but not ARH, increased the steady-state plasma membrane abundance of CFTR in polarized CFBE41o- cells (Fig. 3, *B* and *D*). By contrast, the plasma membrane abundance of CFTR did not increase after partial silencing of the μ2 adaptin (Fig. 3, *B* and *D*). Likewise, silencing the α-adaptin did not increase CFTR abundance in the plasma membrane (Fig. 3*B*). Silencing Dab2 and μ2 together increased the plasma membrane CFTR abundance, similar to silencing Dab2 alone (Fig. 3, *C* and *D*). The increased plasma membrane abundance of CFTR after partial silencing of Dab2 alone or together with μ2 could result, at least in part, from inhibiting CFTR recruitment to CCVs and, thus, CFTR endocytosis. The lack of a significant effect on the plasma membrane abundance of CFTR after partial silencing of μ2 suggests that AP-2 was dispensable for CFTR recruitment to CCVs. Taken together the above results indicate that in polarized human airway epithelial cells, Dab2 may facilitate CFTR recruitment to CCVs via an AP-2 independent mechanism.

The increased plasma membrane abundance of CFTR could result from accelerating translation and targeting CFTR to the plasma membrane or from increasing the plasma membrane stability of CFTR or from both. Thus, we examined the disappearance of biotinylated (*i.e.* plasma membrane) CFTR in polarized CFBE41o- cells over time at 37 °C in the presence of 20 μg/ml cycloheximide to inhibit protein translation. As illus-

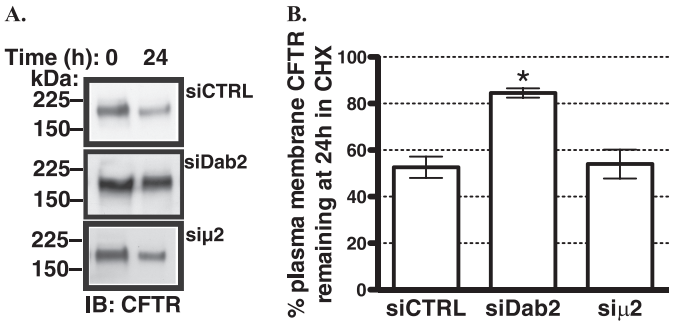

FIGURE 4. **Biotinylation experiments performed to determine the effects of Dab2 and AP-2 on CFTR expression in the plasma membrane of CFBE41o- cells as a function of time.** Shown are representative Western blots (*IB*, *A*) and a summary of experiments (*B*) demonstrating that silencing Dab2 attenuated the disappearance of CFTR from the apical plasma membrane. By contrast, silencing μ2 had no effect on the plasma membrane stability of CFTR. The Dab2 p96 was specifically targeted by the siRNA because, unlike p67, Dab2 p96 functions as an endocytic adaptor. Silencing the μ2 adaptin was used to inhibit the AP-2 complex assembly. CFBE41o- cells were transfected with 50 nM siRNA. Disappearance of CFTR from the plasma membrane was monitored over time in the presence of 20 μg/ml cycloheximide (*CHX*) at 37 °C. In siRNA negative control (*siCTRL*)-treated cells, ~50% of CFTR disappeared from the plasma membrane in 24 h. Thus, data are reported at the 24-h time point. Plasma membrane proteins were isolated by selective apical membrane biotinylation. Ezrin expression in the post-nuclear supernatants was used as a loading control (not shown). *, $p < 0.05$ *versus* time zero in siCTRL. Three experiments/group were performed. *Error bars*, S.E.

trated in Fig. 4, siDab2 increased CFTR stability in the plasma membrane in the presence of cycloheximide. By contrast, siμ2 did not slow the decline in the amount of plasma membrane CFTR in the presence of cycloheximide. These results are consistent with the conclusion that siDab2 increases the plasma membrane abundance of CFTR by a mechanism mediated at least in part by increasing CFTR stability in the plasma membrane and independent of AP-2. Taken together, the above data indicate that in human airway epithelial cells, endogenous Dab2 decreases CFTR abundance in the plasma membrane by reducing the plasma membrane stability of CFTR in an AP-2 independent manner.

Silencing Dab2 Increases CFTR-mediated Cl^- Secretion across Polarized Human Airway Epithelial Cells—CFTR-mediated Cl^- secretion is determined by the activity and number of the plasma membrane CFTR Cl^- channels. Because silencing Dab2 increased the plasma membrane abundance of CFTR, we assayed the functionality of the rescued fraction, predicting that it would also increase CFTR mediated Cl^- secretion. siDab2 but not siμ2 increased the forskolin/IBMX-stimulated Cl^- currents across CFBE41o- monolayers (Fig. 5). These results are consistent with the above data that siDab2 increased CFTR abundance in the plasma membrane and suggest that endogenous Dab2 decreases CFTR-mediated Cl^- secretion by decreasing the amount of CFTR in the plasma membrane in human airway epithelial cells.

Silencing Dab2 Specifically Decreases Clathrin-mediated Endocytosis of CFTR—Based on the known function of Dab2, we anticipated that the effects of siDab2 on CFTR trafficking were due to shifts in endocytic uptake. To test this hypothesis, endocytic assays were conducted to determine the mechanism of increased CFTR abundance and stability in the plasma membrane after silencing Dab2. The siCTRL (non-silencing siRNA) had no effect on CFTR endocytosis as compared with the non-transfected CFBE41o- cells (data not shown). As illustrated in Fig. 6, siDab2 decreased CFTR endocytosis. The reduction in CFTR endocytosis is consistent with the increased plasma membrane stability of CFTR observed in cells transfected with siDab2. By contrast, siμ2 caused only a slight and not statistically significant decrease in CFTR endocytosis. Taken together, these data are consistent with the conclusion that Dab2 facilitates CFTR endocytosis by an AP-2-independent mechanism in polarized human airway epithelial cells.

If Dab2 facilitates CFTR endocytosis by recruiting CFTR to CCVs, silencing Dab2 should inhibit CFTR recruitment and should reduce CFTR abundance in CCVs. To test this prediction, CCV fractions were isolated from polarized CFBE41o- cells by density gradient and differential centrifugation after silencing Dab2. As illustrated in Fig. 7, siDab2 decreased the abundance of CFTR in CCVs. By contrast, siDab2 did not decrease the constitutive abundance of EGFR in CCVs. Conversely, after silencing the μ2 adaptin, the CCV abundance of EGFR was reduced, whereas that of CFTR was not significantly affected. Taken together these data demonstrate that Dab2 specifically promotes CFTR recruitment to CCVs and facilitates CFTR endocytosis in polarized human airway epithelial cells. Because AP-2 is critical for optimal CCV formation and AP-2 depletion decreases the number of CCVs, the above data demonstrate that Dab2 is capable of sustaining CFTR endocytosis even if the overall number of CCVs is reduced.

CFTR ^{1424}YDSI Motif Is Not Essential for CFTR Endocytosis in Human Airway Epithelial Cells—CFTR interacts directly with μ2 *in vitro*, and the interaction is critical for efficient CFTR endocytosis in non-epithelial cells. The above silencing studies demonstrate that moderate depletion of AP-2 does not attenuate CFTR endocytosis, suggesting that AP-2 is not essential for CFTR recruitment to CCVs and because CFTR recruitment is promoted and sustained by Dab2. However, it cannot be excluded that due to partial silencing, the μ2 abundance is sufficient for CFTR recruitment to CCVs and its endocytosis. Hence, studies were conducted to examine whether the interaction between CFTR and μ2 is essential for CFTR endocytosis in human airway epithelial cells. First, we examined whether the Y1424A substitution in CFTR, previously shown to disrupt the CFTR-μ2 interaction, affects CFTR recruitment to CCVs. Parental CFBE41o- cells transiently transfected with the GFP-CFTR WT or the GFP-CFTR Y1424A mutant were grown in plastic tissue culture dishes for 72 h. Cells were lysed, and the CCV fractions were isolated by density gradient and differential centrifugation. As illustrated in Fig. 8, the abundance of the GFP-CFTR WT and GFP-CFTR Y1424A in CCVs was similar.

Next, we examined the effect of the Y1424A substitution on CFTR endocytosis. The biotinylation-based endocytic assays were conducted in parental CFBE41o- cells expressing GFP-CFTR WT or the GFP-CFTR Y1424A mutant. As illustrated in Fig. 9, endocytosis of the GFP-CFTR WT and GFP-CFTR Y1424A was similar in the linear uptake phase, consistent with steady-state measurements (Figs. 8 and 10).

Finally, studies were conducted to determine the effect of the Y1424A substitution on CFTR stability in the plasma membrane. Parental CFBE41o- cells were treated with 20 μg/ml cycloheximide to inhibit protein translation. After plasma

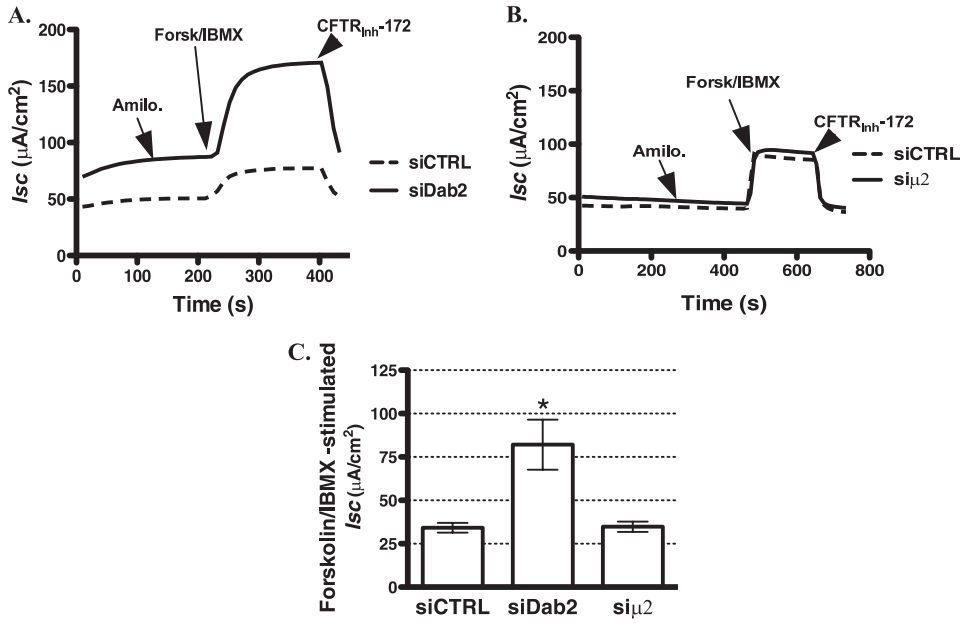

FIGURE 5. **Ussing chamber experiments performed to determine the effects of Dab2 and AP-2 on the CFTR mediated Cl^- secretion across CFBE41o- monolayers.** Cells were transfected with 50 nM siRNA. The Dab2 p96 was specifically targeted by the siRNA because, unlike p67, Dab2 p96 functions as an endocytic adaptor. Silencing the μ2 adaptin was used to inhibit the AP-2 complex assembly. CFBE41o- cells were bathed in solutions with apical-to-basolateral Cl^- gradient in the presence of amiloride (100 μM) in the apical bath solution to inhibit Na^+ absorption through ENaC. *Isc* was stimulated with forskolin (20 μM), and IBMX (50 μM) was added to the apical and basolateral bath solution. Thiazolidonone $CFTR_{inh}$-172 (20 μM) was added to the apical bath solution to inhibit CFTR-mediated *Isc*. Data are expressed as net stimulated *Isc*, calculated by subtracting the base-line *Isc* from the peak stimulated *Isc*. The siRNA negative control (*siCTRL*) did not affect the forskolin/IBMX-stimulated *Isc* across CFBE41o-cells compared with the non-transfected cells (data not shown). Silencing Dab2 increased the forskolin/IBMX-stimulated *Isc* across CFBE41o-cells (*A* and *C*). By contrast, silencing μ2 did not increase the forskolin/IBMX-stimulated *Isc* across CFBE41o-cells (*B* and *C*). *, $p < 0.05$ *versus* siCTRL. Shown are 18 monolayers/group in *A* and 12 monolayers/group in *B* each from three different cultures. *Error bars*, S.E.

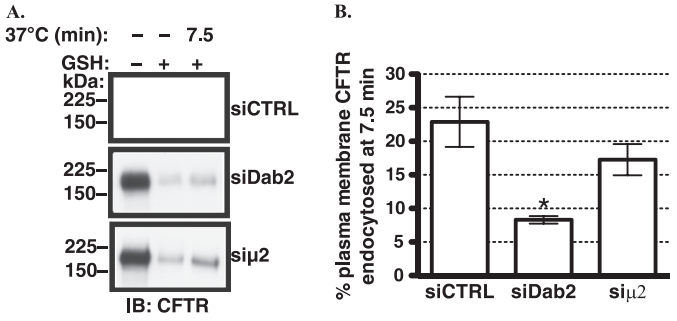

FIGURE 6. **Endocytic assays performed to determine the effects of Dab2 and AP-2 on CFTR endocytosis in CFBE41o- cells.** Cells were transfected with 50 nM siRNA. The Dab2 p96 was specifically targeted by the siRNA because, unlike p67, Dab2 p96 functions as an endocytic adaptor. Silencing the μ2 adaptin was used to inhibit the AP-2 complex assembly. CFTR endocytosis was linear up to 7.5 min and was not affected by the siRNA negative control (*siCTRL*); thus, data are reported at the 7.5-min time point (14). Representative Western blots (*A*) and summary of experiments (*B*) demonstrating that siDab2 decreased CFTR endocytosis. By contrast, siμ2 did not decrease CFTR endocytosis. The amount of biotinylated CFTR remaining after the GSH treatment at 4 °C without warming to 37 °C was considered background and was subtracted from the amount of biotinylated CFTR remaining after warming to 37 °C at each time point. CFTR endocytosis was calculated after subtraction of the background (see above) and was expressed as the percent of CFTR remaining biotinylated before and after warming to 37 °C. Ezrin expression in the post-nuclear supernatants was used as a loading control (data not shown). *, $p < 0.05$ *versus* siCTRL. Four experiments/group were performed. *Error bars*, S.E.

membrane biotinylation at 4 °C, the disappearance of the GFP-CFTR WT or GFP-CFTR Y1424A mutant from the plasma membrane was monitored as a function of time at 37 °C. As shown in Fig. 10, the plasma membrane stability of the GFP-CFTR WT and GFP-CFTR Y1424A was similar.

The above data demonstrate that the Y1424A mutation affects neither CFTR recruitment to CCVs, CFTR endocytosis, nor CFTR stability in the plasma membrane and suggest that the CFTR interaction with μ2 adaptin is not essential for CFTR endocytosis in human airway epithelial cells. These data further support the view that Dab2 facilitates CFTR recruitment to CCVs and CFTR endocytosis by an AP-2 independent mechanism.

Dab2 DH Domain Interacts with CFTR—Previous studies demonstrated that Dab2 does not require interaction with AP-2 to mediate endocytosis of proteins that bind to the N-terminal Dab2 DH domain. If Dab2 mediates CFTR endocytosis by an AP-2 independent mechanism, CFTR would be expected to interact with the DH domain. The fragment spanning amino acids 1–205 contains the DH domain (Dab2 DH) and interacts with proteins containing the NP*X*Y motif, such as the amyloid precursor protein (APP) and LDLR, and with phosphoinositides in the plasma membrane but not with clathrin or AP-2 (27). First, fluorescence binding assays were performed to confirm that affinity-purified recombinant Dab2 DH binds the fluorescein-tagged, APP-derived NP*X*Y peptide (*F**-APP10) with high affinity ($K_d \sim 10$ μM; Fig. 11*A*). By contrast, the amino acid substitutions in the NP*X*Y binding pocket, previously shown to disrupt the DH domain interactions with NP*X*Y motifs, S122T/H144F (Dab2 DH 122/144), severely impaired peptide binding (Ref. 27; $K_d > 1$ mM; Fig. 11*A*).

Next, studies were conducted to determine whether CFTR interacts with the Dab2 DH domain. CFBE41o- cells stably expressing WT-CFTR were transfected with the GFP-Dab2

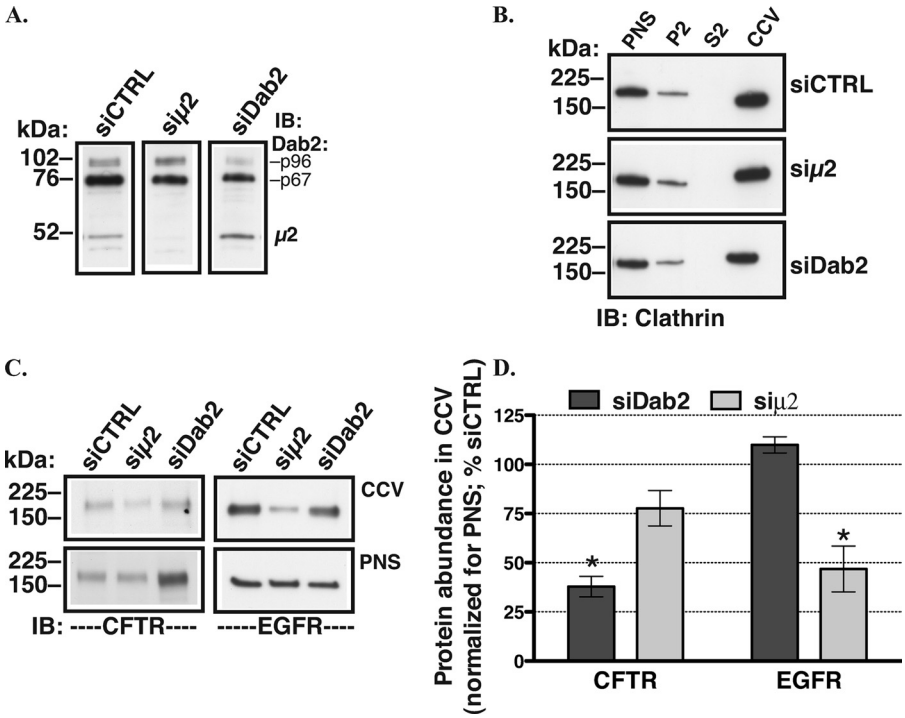

FIGURE 7. **Subcellular fractionation experiments performed to determine the effects of Dab2 and AP-2 on CFTR recruitment to the CCV in polarized CFBE41o- cells.** The CCV fractions were prepared by density gradient and differential centrifugation in CFBE41o- cells transfected with 50 nM siRNA. The Dab2 p96 was specifically targeted by the siDab2 because, unlike p67, Dab2 p96 functions as an endocytic adaptor. Silencing the μ2 adaptin was used to inhibit the AP-2 complex assembly. *A*, a representative Western blot (*IB*) demonstrates that siDab2 decreased the Dab2 p96 protein abundance in PNS without decreasing abundance of the μ2 adaptin, and siμ2 decreased the μ2 protein abundance without decreasing abundance of Dab2. *B*, representative Western blots demonstrate successful isolation of CCVs as demonstrated by the enrichment of clathrin in the CCV fractions. *P2*, cytosolic fraction; *S2*, microsomal fraction. The CCV abundance of clathrin normalized to PNS was similar in cells transfected with siCTRL, siμ2, and siDab2. A representative Western blot (*C*) and summary of experiments (*D*) demonstrates that siDab2 decreased the abundance of CFTR in CCVs relative to siCTRL levels. By contrast, siDab2 did not decrease the constitutive abundance of EGFR in CCVs. Unlike EGFR, the CCV abundance of CFTR was not significantly decreased after silencing the μ2 adaptin. The plasma membrane abundance of CFTR and EGFR were normalized for PNS abundance of the respective protein (*C*). *, $p < 0.05$ *versus* siRNA negative control (*siCTRL*). Three experiments/group were performed. *Error bars*, S.E.

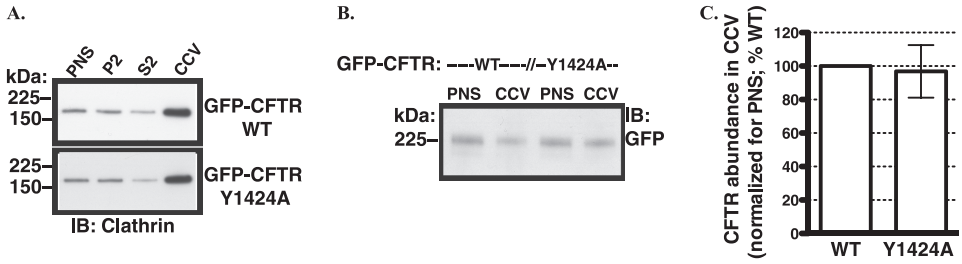

FIGURE 8. **Subcellular fractionation experiments performed to determine the effect of the Y1424A mutation on CFTR recruitment CCV in CFBE41o- cells.** The CCV fractions were prepared by density gradient and differential centrifugation in parental CFBE41o- cells 72 h after transfection with the GFP-CFTR WT or GFP-CFTR Y1424A mutant. *A*, a representative Western blot (*IB*) demonstrates successful isolation of CCVs as demonstrated by the enrichment of clathrin in the CCV fractions. *P2*, cytosolic fraction; *S2*, microsomal fraction. A representative Western blot (B) and summary of experiments (*C*) demonstrate that the Y1424A mutation did not decrease the abundance of CFTR in CCVs. The CCV abundance of CFTR was normalized for the abundance of CFTR in PNS. Three experiments/group were performed. *Error bars*, S.E.

DH, GFP-Dab2 DH 122/144, or vector control (CTRL). Western blot analysis of the immunoprecipitated protein complexes demonstrated that only the GFP-Dab2 DH fragment co-immunoprecipitated with CFTR (Fig. 11*B*). These data are consistent with the conclusion that in human airway epithelial cells, CFTR interacts with the Dab2 DH domain by a mechanism dependent on the peptide binding pocket.

Dab2 DH Domain Inhibits CFTR Endocytosis—If Dab2 interacts with CFTR via the DH domain, we hypothesize that the GFP-Dab2 DH fragment, which is deficient in clathrin binding, should compete with the endogenous Dab2 for cargo (CFTR) and thus inhibit CFTR endocytosis. As illustrated in Fig. 12, the GFP-Dab2 DH decreased CFTR endocytosis. By contrast, the GFP-Dab2 DH 122/144 mutant did not inhibit CFTR endocytosis. The dependence of the dominant negative effect of the GFP-Dab2 DH fragment on a functional peptide binding pocket demonstrates that Dab2 facilitates CFTR endocytosis by a mechanism that involves interaction with the NP*X*Y recognition site.

F-APP10 Peptide Increases CFTR Abundance in Plasma Membrane*—Studies were conducted to determine the effect of blocking the DH peptide binding pocket in Dab2 on CFTR abundance in the plasma membrane. The *F**-APP10 peptide and the BioPORTER Protein Delivery reagent were added to

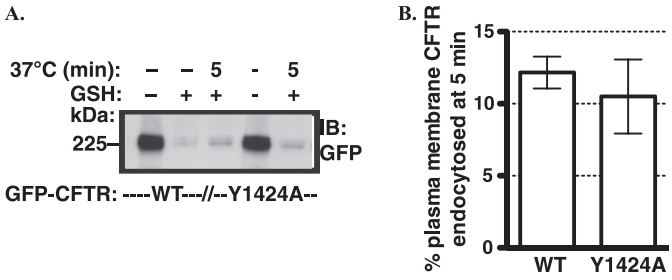

FIGURE 9. **Endocytic assays performed to determine the effect of the Y1424A mutation on CFTR endocytosis.** Endocytic assays were performed in parental CFBE41o- cells 72 h after transfection with the GFP-CFTR WT or GFP-CFTR Y1424A mutant. Endocytosis of the GFP-CFTR WT was linear up to 5 min (data not shown); thus, data are reported at the 5-min time point. A representative Western blot (*IB*; *A*) and summary of experiments (*B*) demonstrates that the Y1424A mutation did not inhibit CFTR endocytosis. The amount of biotinylated CFTR remaining after the GSH treatment at 4 °C without warming to 37 °C was considered background and was subtracted from the amount of biotinylated CFTR remaining after warming to 37 °C for 5 min. CFTR endocytosis was calculated after subtraction of the background (see above) and was expressed as the percent of CFTR remaining biotinylated before and after warming to 37 °C. The endocytosis of transiently transfected GFP-CFTR WT was linear up to 5 min in the parental CFBE41o- cells (data not shown); therefore, the 5-min time point data are reported. Ezrin expression in the post-nuclear supernatants was used as a loading control (data not shown). Three experiments/group were performed. *Error bars*, S.E.

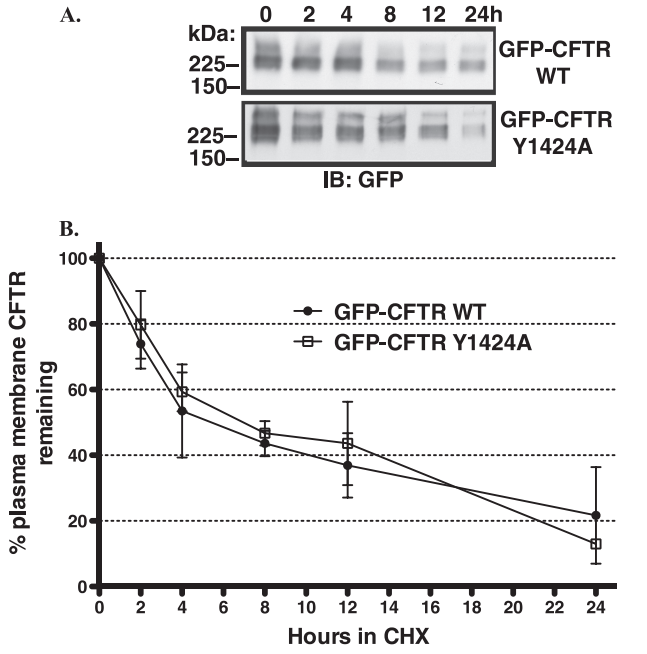

FIGURE 10. **Biotinylation experiments performed to determine the effects of the Y1424A mutation on CFTR expression in the plasma membrane of CFBE41o- cells as a function of time.** Biotinylation experiments were performed in parental CFBE41o- cells 72 h after transfection with the GFP-CFTR WT or GFP-CFTR Y1424A mutant. Disappearance of CFTR from the plasma membrane was monitored over time in the presence of 20 μg/ml cycloheximide (*CHX*) at 37 °C. A representative Western blot (*IB*; *A*) and summary of experiments (*B*) demonstrate that the Y1424A mutation did not increase CFTR stability in the plasma membrane. Plasma membrane proteins were isolated by selective plasma membrane biotinylation. Ezrin expression in the post-nuclear supernatants was used as a loading control (data not shown). Three experiments/group were performed. *Error bars*, S.E.

the apical chamber of polarized CFBE41o- cells. Internalization of the *F**-APP10 peptide was demonstrated by detection of the fluorescein tag inside the cells after a 30-min incubation (Fig. 13*A*). The *F**-APP10 peptide is expected to inhibit endocytosis and increase the plasma membrane abundance of endogenous cargo proteins, such as LDLR, by competing with these proteins for binding to Dab2. As expected, the *F**-APP10 peptide increased the abundance of LDLR in the apical plasma membrane (Fig. 13*B*). Similar to LDLR, the apical plasma membrane abundance of CFTR was increased by the *F**-APP10 peptide compared with vehicle control (Fig. 13*B*). The effect of the *F**-APP10 peptide on the plasma membrane CFTR is consistent with the dominant negative effect of the GFP-Dab2 DH fragment on CFTR endocytosis. Taken together the above data demonstrate a novel interaction between CFTR and Dab2 via the DH domain amenable to regulation with an NP*X*Y peptide.

DISCUSSION

The major novel observation in this study is that in polarized human airway epithelial cells, Dab2 mediates AP-2-independent recruitment of CFTR to CCVs. As a result, it facilitates CFTR endocytosis and reduces CFTR abundance and stability in the plasma membrane. These effects are mediated by the DAB homology domain. Moreover, we show that AP-2 is not essential for CFTR recruitment to CCVs in these cells.

Several lines of evidence in this study support these conclusions. Compared with controls, partial silencing of Dab2 led to an increase in steady-state CFTR plasma membrane abundance, CFTR plasma membrane stability, and CFTR-mediated Cl^- secretion. Dab2 depletion also decreased both CFTR abundance in the CCV fraction and CFTR endocytosis. Similar levels of μ2 silencing and a corresponding loss of AP-2 had no significant effect on any of these CFTR trafficking or stability characteristics (Figs. 3- 7). Targeted disruption by mutagenesis of the direct interaction between CFTR and μ2 also did not attenuate CFTR recruitment to CCVs, CFTR endocytosis, or CFTR stability in the plasma membrane (Figs. 8–10).

Furthermore, CFTR co-immunoprecipitated with the GFP-Dab2 DH fragment, which did not interact with either AP-2 or clathrin (Fig. 11). Overexpression of the GFP-Dab2 DH fusion protein reduced CFTR abundance in the CCV fraction and CFTR endocytosis in a dominant negative manner (Fig. 12). Finally, the plasma membrane abundance of CFTR was increased, similar to that of LDLR, by the NP*X*Y peptide, *F**-APP10, which specifically binds to the DH peptide-binding site (Figs. 11 and 13).

Another study has shown a role for AP-2 in CFTR endocytosis in human airway epithelial cells (19). Because AP-2 mediates both clathrin coat assembly and cargo protein recruitment to CCVs (17), the high level of knockdown observed in the previous study (~90% of μ2) would have compromised both functions and, therefore, could not distinguish between them. In contrast, in HEK293 cells, where AP-2 is known to play a role in CFTR recruitment, a more modest 64% knockdown was sufficient to cause a significant decrease in CFTR endocytosis (18) by preferentially targeting the recruiting step. Utilizing a similarly limited knockdown (~ 60% of μ2 adaptin) in airway epithelial cells, we see no difference in either the CFTR content in CCVs or CFTR endocytosis (Figs. 6 and 7). Thus, we conclude that during CFTR endocytosis AP-2 is necessary for the clathrin coat assembly but is largely dispensable for CFTR recruitment to the clathrin coats.

Consistent with this model, the previously reported 10-fold knockdown of AP-2 only caused a 2-fold reduction in CFTR

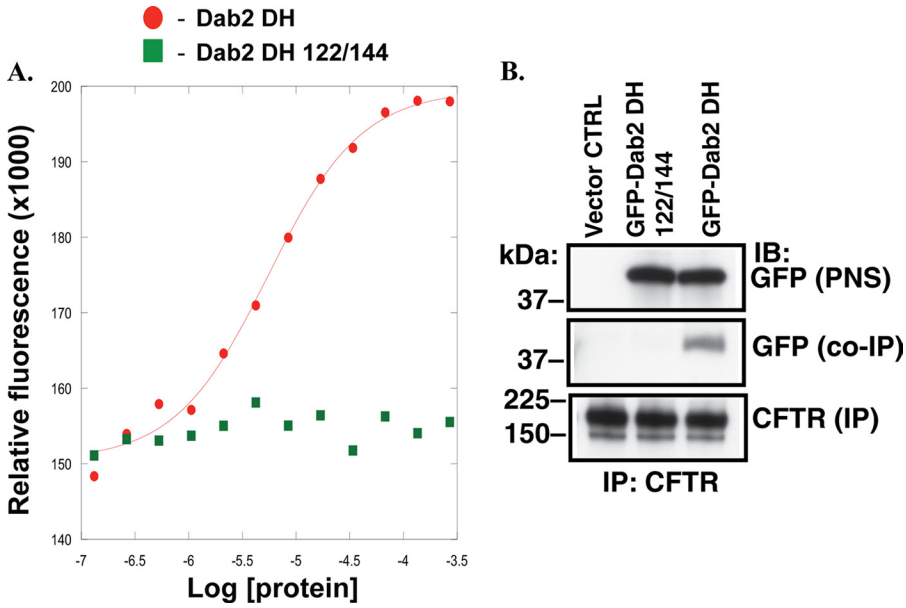

FIGURE 11. **Representative experiments demonstrating the interaction between the Dab2 DH domain and CFTR in CFBE41o-.** The Dab2 DH domain contains an NP*X*Y binding pocket that interacts with the NP*X*Y domains in cargo proteins. *A*, fluorescence binding assays were performed to confirm that the affinity-purified recombinant Dab2 DH fragment interacts with the fluorescein-tagged, APP-derived peptide (*F**-APP10) with high affinity ($K_d \sim 10\ \mu$M). By contrast, the S122T/H144F substitutions in the Dab2 DH fragment (*Dab2 DH 122/144*) severely impaired peptide binding ($K_d > 1$ mM). Three experiments/group were performed. *B*, immunoprecipitation (*IP*) experiments were performed to examine whether CFTR interacts with the Dab2 DH domain and whether the interaction depends on the NP*X*Y binding pocket in the Dab2 DH domain. CFBE41o- cells stably expressing WT-CFTR were transfected with the vector control (*CTRL*), GFP-Dab2 DH, or the GFP-Dab2 DH S122T/H144F (*122/144*). CFTR was immunoprecipitated with antibody M3A7 (CFTR (IP)). Western blot (*IB*) analysis of the immunoprecipitated protein complexes demonstrated that only the GFP-Dab2 DH fragment co-immunoprecipitated with CFTR (GFP (co-IP)). Proteins were separated by SDS-PAGE using 7.5% gels (2% of the whole cell lysates run on gel). Experiments were repeated three times from separate cultures with similar results.

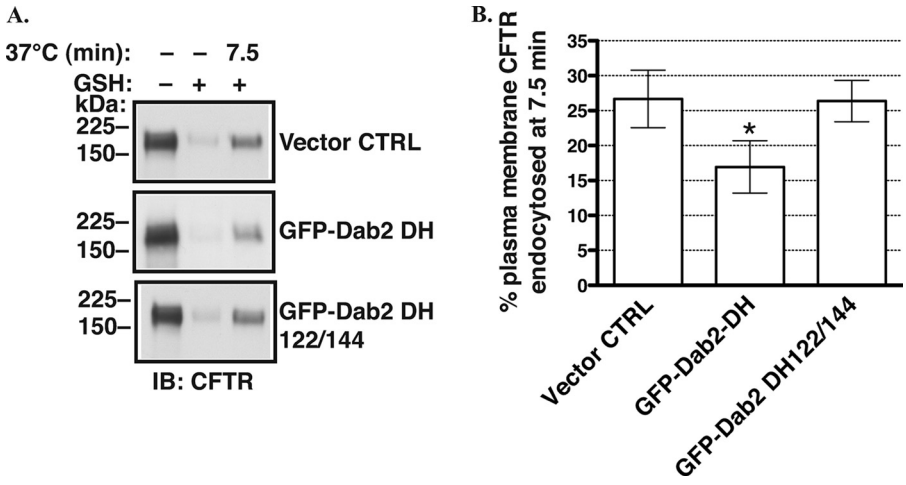

FIGURE 12. **Endocytic assays performed to determine the effects of the Dab2 DH domain on CFTR endocytosis in CFBE41o- cells.** CFBE41o- cells stably expressing WT-CFTR were transfected with the vector control (*CTRL*), GFP-Dab2 DH, or the GFP-Dab2 DH S122T/H144F (*122/144*), and the endocytic assays were performed 72 h after transfection. Representative Western blots (*IB*, *A*) and summary of experiments (*B*) demonstrate that the GFP-Dab2 DH decreased CFTR endocytosis. By contrast, the GFP-Dab2 DH 122/144 mutant did not inhibit CFTR endocytosis. The amount of biotinylated CFTR remaining after the GSH treatment at 4 °C without warming to 37 °C was considered background and was subtracted from the amount of biotinylated CFTR remaining after warming to 37 °C at each time point. CFTR endocytosis was calculated after subtraction of the background (see above) and was expressed as the percent of CFTR remaining biotinylated before and after warming to 37 °C. CFTR endocytosis was linear up to 7.5 min (14); thus, results are reported at the 7.5-min time point. Ezrin expression in the post-nuclear supernatants was used as a loading control (data not shown). *, $p < 0.05$ *versus* vector CTRL. Three experiments/group were performed. *Error bars*, S.E.

endocytosis in airway epithelial cells (19). Based on the studies of Motley *et al.* (17), this behavior suggests that CFTR has privileged access to the remaining CCVs. Our data demonstrate that Dab2 can provide CFTR with such privileged access to the existing CCVs after AP-2 depletion. Such access has been demonstrated for the LDLR, which contains an NP*X*Y motif that enables it to interact with Dab2 (17). In agreement with this model, Fu *et al.* (19) also showed that silencing Dab2 impedes CFTR endocytic uptake, although the interaction of Dab2 with CFTR remained unclear, as it does not contain a recognized Dab2 binding motif.

Against this background, our data provide compelling evidence that the Dab2 NP*X*Y peptide-binding site nevertheless plays a critical role in CFTR recruitment. Mutation of the bind-

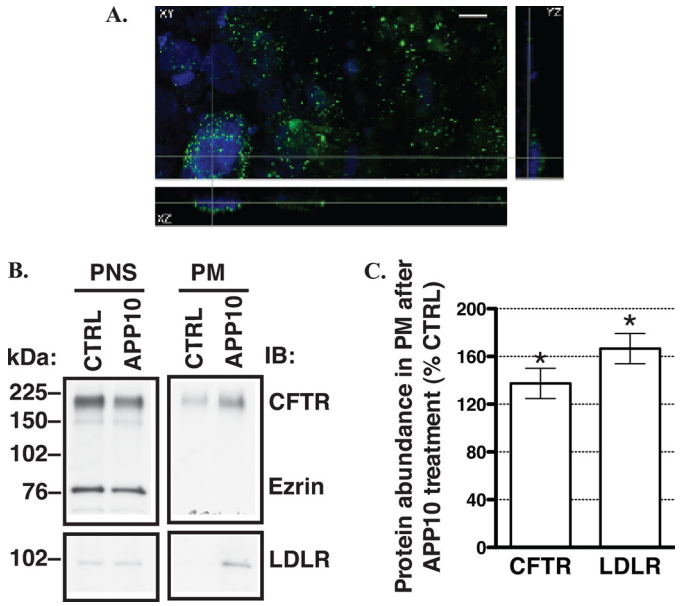

FIGURE 13. **Experiments performed to determine the effect of blocking the Dab2 peptide binding pocket on CFTR abundance in the plasma membrane.** The *F**-APP10 peptide (1.25 mM) in DMSO or vehicle control (*CTRL*) and the BioPORTER® protein delivery reagent were added to the apical side of the monolayers and incubated at 37 °C for 30 min in the cell culture incubator. *A*, confocal microscopy images demonstrate intracellular localization of the *F**-APP10 peptide in CFBE41o- cells. After the incubation with *F**-APP10, monolayers were thoroughly washed at 4 °C, fixed with 2% paraformaldehyde, and mounted onto slides with ProLong Gold Antifade reagent with DAPI. The N-terminally located fluorescein tag on the internalized *F**-APP10 peptide was excited at the 488-nm spectral line of the multiline argon laser. A representative z-stack is shown in the *xy*, *xz*, and *yz* projection. No fluorescence signal was observed in cells incubated with the vehicle control (not shown). *Error bar* = 10 μm. Representative Western blots (*IB*, *B*) and a summary of experiments (*C*) demonstrate that similar to LDLR, CFTR abundance was increased in the apical plasma membrane (*PM*) after incubation with the *F**-APP10 peptide compared with the vehicle CTRL. The *F**-APP10 peptide did not change the abundance of CFTR or LDLR in the PNS. Moreover, the *F**-APP10 peptide did not change the abundance of ezrin in the PNS (90.3 ± 7.1% *versus* CTRL; $n = 5$; p = not significant). The absence of ezrin in the biotinylated fraction (*B*) confirms that only plasma membrane proteins were biotinylated. The plasma membrane proteins were isolated by selective apical plasma membrane biotinylation. *, $p < 0.05$ *versus* CTRL. Four-five experiments/group were performed. *Error bars*, S.E.

ing site abrogates the dominant negative endocytic effect of the GFP-Dab2 DH fusion protein (Fig. 12). More importantly, an NP*X*Y-containing peptide that binds specifically to the DH domain increases CFTR cell surface abundance in analogy to Dab2 silencing (Fig. 13).

Because CFTR does not contain a canonical NP*X*Y motif, we predict that CFTR may interact indirectly via another endocytic adaptor or membrane receptor containing the NP*X*Y motif that binds to the Dab2 DH domain. Alternatively, CFTR may interact with Dab2 via a non-canonical signal. Future studies will be required to elucidate the details of these interactions in the context of airway epithelial cells, particularly given the tissue and polarization dependence of endocytic adaptor complex formation. For example, in non-epithelial cells the interaction between CFTR and μ2 was necessary for efficient CFTR endocytosis (10, 20, 21). By contrast, we found the interaction between CFTR and μ2 to be dispensable for CFTR recruitment and endocytosis in polarized human airway epithelial cells.

Regardless of the exact molecular complexes involved, the effect of the *F**-APP10 peptide in this study strongly suggests that compounds containing the NP*X*Y sequence can regulate CFTR abundance in the plasma membrane. Such compounds do not target the AP-2 mediated interactions and thus should not decrease the number of CCVs nor globally inhibit protein endocytosis. Because rescued ΔF508-CFTR has limited plasma membrane stability, we propose that regulating the CFTR-Dab2 interaction may provide useful biochemical tools to investigate the stability defect as well as uncovering future pharmacological approaches to correct it.

Acknowledgments—We thank Dr. John Wakefield from Tranzyme, Inc. (Birmingham, AL) who generated the CFBE41o- cells stably expressing the WT-CFTR and Dr. J.P. Clancy from the University of Alabama at Birmingham for providing the stable CFBE41o- cells. We thank Dr. Bruce A. Stanton from Dartmouth Medical School for the CFTR plasmids and for insightful review of the manuscript. Moreover, we thank Dr. Amitava Mukherjee and Laura Nwranski from the University of Pittsburgh for technical assistance with the experiments.

REFERENCES

1. Riordan, J. R., Rommens, J. M., Kerem, B., Alon, N., Rozmahel, R., Grzelczak, Z., Zielenski, J., Lok, S., Plavsic, N., and Chou, J. L. (1989) Identification of the cystic fibrosis gene. Cloning and characterization of complementary DNA. *Science* **245,** 1066–1173
2. Rommens, J. M., Iannuzzi, M. C., Kerem, B., Drumm, M. L., Melmer, G., Dean, M., Rozmahel, R., Cole, J. L., Kennedy, D., and Hidaka, N. (1989) Identification of the cystic fibrosis gene. Chromosome walking and jumping. *Science* **245,** 1059–1065
3. Howard, M., Jiang, X., Stolz, D. B., Hill, W. G., Johnson, J. A., Watkins, S. C., Frizzell, R. A., Bruton, C. M., Robbins, P. D., and Weisz, O. A. (2000) Forskolin-induced apical membrane insertion of virally expressed, epitope-tagged CFTR in polarized MDCK cells. *Am. J. Physiol. Cell Physiol.* **279,** C375–C382
4. Boucher, R. C. (2004) New concepts of the pathogenesis of cystic fibrosis lung disease. *Eur. Respir. J.* **23,** 146–158
5. Tarran, R., Button, B., and Boucher, R. C. (2006) Regulation of normal and cystic fibrosis airway surface liquid volume by phasic shear stress. *Annu. Rev. Physiol.* **68,** 543–561
6. Bertrand, C. A., and Frizzell, R. A. (2003) The role of regulated CFTR trafficking in epithelial secretion. *Am. J. Physiol. Cell Physiol.* **285,** C1–C18
7. Guggino, W. B., and Stanton, B. A. (2006) New insights into cystic fibrosis. Molecular switches that regulate CFTR. *Nat. Rev. Mol. Cell Biol.* **7,** 426–436
8. Riordan, J. R. (2008) CFTR function and prospects for therapy. *Annu. Rev. Biochem.* **77,** 701–726
9. Lukacs, G. L., Segal, G., Kartner, N., Grinstein, S., and Zhang, F. (1997) Constitutive internalization of cystic fibrosis transmembrane conductance regulator occurs via clathrin-dependent endocytosis and is regulated by protein phosphorylation. *Biochem. J.* **328,** 353–361
10. Prince, L. S., Peter, K., Hatton, S. R., Zaliauskiene, L., Cotlin, L. F., Clancy, J. P., Marchase, R. B., and Collawn, J. F. (1999) Efficient endocytosis of the cystic fibrosis transmembrane conductance regulator requires a tyrosine-based signal. *J. Biol. Chem.* **274,** 3602–3609 ***9920908***
11. Sharma, M., Pampinella, F., Nemes, C., Benharouga, M., So, J., Du, K., Bache, K. G., Papsin, B., Zerangue, N., Stenmark, H., and Lukacs, G. L. (2004) Misfolding diverts CFTR from recycling to degradation. Quality control at early endosomes. *J. Cell Biol.* **164,** 923–933
12. Swiatecka-Urban, A., Brown, A., Moreau-Marquis, S., Renuka, J., Coutermarsh, B., Barnaby, R., Karlson, K. H., Flotte, T. R., Fukuda, M., Langford, G. M., and Stanton, B. A. (2005) The short apical membrane half-life of rescued F508-cystic fibrosis transmembrane conductance regulator (CFTR) results from accelerated endocytosis of ΔF508-CFTR in polarized human airway epithelial cells. *J. Biol. Chem.* **280,** 36762–36772
13. Cushing, P. R., Vouilleme, L., Pellegrini, M., Boisguerin, P., and Madden,

D. R. (2010) A stabilizing influence. CAL PDZ inhibition extends the half-life of ΔF508-CFTR. *Angew. Chem. Int. Ed. Engl.* **49,** 9907–9911
14. Ye, S., Cihil, K., Stolz, D. B., Pilewski, J. M., Stanton, B. A., and Swiatecka-Urban, A. (2010) c-Cbl facilitates endocytosis and lysosomal degradation of cystic fibrosis transmembrane conductance regulator in human airway epithelial cells. *J. Biol. Chem.* **285,** 27008–27018
15. Okiyoneda, T., and Lukacs, G. L. (2007) Cell surface dynamics of CFTR. The ins and outs. *Biochim. Biophys. Acta* **1773,** 476–479
16. Traub, L. M. (2003) Sorting it out.AP-2 and alternate clathrin adaptors in endocytic cargo selection. *J. Cell Biol.* **163,** 203–208
17. Motley, A., Bright, N. A., Seaman, M. N., and Robinson, M. S. (2003) Clathrin-mediated endocytosis in AP-2-depleted cells. *J. Cell Biol.* **162,** 909–918
18. Collaco, A., Jakab, R., Hegan, P., Mooseker, M., and Ameen, N. (2010) αAP-2 directs myosin VI-dependent endocytosis of cystic fibrosis transmembrane conductance regulator chloride channels in the intestine. *J. Biol. Chem.* **285,** 17177–17187
19. Fu, L., Rab, A., Tang, L. P., Rowe, S. M., Bebok, Z., and Collawn, J. F. (2012) Dab2 is a key regulator of endocytosis and post-endocytic trafficking of the cystic fibrosis transmembrane conductance regulator. *Biochem. J.* **441,** 633–643
20. Weixel, K. M., and Bradbury, N. A. (2000) The carboxyl terminus of the cystic fibrosis transmembrane conductance regulator binds to AP-2 clathrin adaptors. *J. Biol. Chem.* **275,** 3655–3360
21. Weixel, K. M., and Bradbury, N. A. (2001) μ2 binding directs the cystic fibrosis transmembrane conductance regulator to the clathrin-mediated endocytic pathway. *J. Biol. Chem.* **276,** 46251–46259
22. Hu, W., Howard, M., and Lukacs, G. L. (2001) Multiple endocytic signals in the C-terminal tail of the cystic fibrosis transmembrane conductance regulator. *Biochem. J.* **354,** 561–572
23. Swiatecka-Urban, A., Boyd, C., Coutermarsh, B., Karlson, K. H., Barnaby, R., Aschenbrenner, L., Langford, G. M., Hasson, T., and Stanton, B. A. (2004) Myosin VI regulates endocytosis of the cystic fibrosis transmembrane conductance regulator. *J. Biol. Chem.* **279,** 38025–38031
24. Hentchel-Franks, K., Lozano, D., Eubanks-Tarn, V., Cobb, B., Fan, L., Oster, R., Sorscher, E., and Clancy, J. P. (2004) Activation of airway cl- secretion in human subjects by adenosine. *Am. J. Respir. Cell Mol. Biol.* **31,** 140–146
25. Chang, C., Wang, X., and Caldwell, R. B. (1997) Serum opens tight junctions and reduces ZO-1 protein in retinal epithelial cells. *J. Neurochem.* **69,** 859–867
26. Kues, W. A., Anger, M., Carnwath, J. W., Paul, D., Motlik, J., and Niemann, H. (2000) Cell cycle synchronization of porcine fetal fibroblasts. Effects of serum deprivation and reversible cell cycle inhibitors. *Biol. Reprod.* **62,** 412–419
27. Yun, M., Keshvara, L., Park, C. G., Zhang, Y. M., Dickerson, J. B., Zheng, J., Rock, C. O., Curran, T., and Park, H. W. (2003) Crystal structures of the Dab homology domains of mouse disabled 1 and 2. *J. Biol. Chem.* **278,** 36572–36581
28. Girard, M., Allaire, P. D., Blondeau, F., and McPherson, P. S. (2005) Isolation of clathrin-coated vesicles by differential and density gradient centrifugation. *Curr. Protoc. Cell Biol.*, Chapter 3, Unit 3.13
29. Swiatecka-Urban, A., Duhaime, M., Coutermarsh, B., Karlson, K. H., Collawn, J., Milewski, M., Cutting, G. R., Guggino, W. B., Langford, G., and Stanton, B. A. (2002) PDZ domain interaction controls the endocytic recycling of the cystic fibrosis transmembrane conductance regulator. *J. Biol. Chem.* **277,** 40099–40105
30. Watts, C., and Davidson, H. W. (1988) Endocytosis and recycling of specific antigen by human B cell lines. *EMBO J.* **7,** 1937–1145
31. Swiatecka-Urban, A., Talebian, L., Kanno, E., Moreau-Marquis, S., Coutermarsh, B., Hansen, K., Karlson, K. H., Barnaby, R., Cheney, R. E., Langford, G. M., Fukuda, M., and Stanton, B. A. (2007) Myosin Vb is required for trafficking of the cystic fibrosis transmembrane conductance regulator in Rab11a-specific apical recycling endosomes in polarized human airway epithelial cells. *J. Biol. Chem.* **282,** 23725–23736
32. Swiatecka-Urban, A., Moreau-Marquis, S., Maceachran, D. P., Connolly, J. P., Stanton, C. R., Su, J. R., Barnaby, R., O'toole, G. A., and Stanton, B. A. (2006) *Pseudomonas aeruginosa* inhibits endocytic recycling of CFTR in polarized human airway epithelial cells. *Am. J. Physiol. Cell Physiol.* **290,** C862–C872
33. Xu, X. X., Yang, W., Jackowski, S., and Rock, C. O. (1995) Cloning of a novel phosphoprotein regulated by colony-stimulating factor 1 shares a domain with the *Drosophila* disabled gene product. *J. Biol. Chem.* **270,** 14184–14191
34. Morris, S. M., and Cooper, J. A. (2001) Disabled-2 colocalizes with the LDLR in clathrin-coated pits and interacts with AP-2. *Traffic* **2,** 111–123
35. Mishra, S. K., Keyel, P. A., Hawryluk, M. J., Agostinelli, N. R., Watkins, S. C., and Traub, L. M. (2002) Disabled-2 exhibits the properties of a cargo-selective endocytic clathrin adaptor. *EMBO J.* **21,** 4915–4926
36. Meyer, C., Zizioli, D., Lausmann, S., Eskelinen, E. L., Hamann, J., Saftig, P., von Figura, K., and Schu, P. (2000) μ1A-adaptin-deficient mice. Lethality, loss of AP-1 binding, and rerouting of mannose 6-phosphate receptors. *EMBO J.* **19,** 2193–2203
37. Peden, A. A., Rudge, R. E., Lui, W. W., and Robinson, M. S. (2002) Assembly and function of AP-3 complexes in cells expressing mutant subunits. *J. Cell Biol.* **156,** 327–336